

## Enzymatic reduction-resistant nitroxyl spin probes with spirocyclohexyl rings

SHOKO OKAZAKI<sup>1</sup>, MD ABDUL MANNAN<sup>2</sup>, KEIJIRO SAWAI<sup>2</sup>, TOSHIKI MASUMIZU<sup>1</sup>, YOZO MIURA<sup>2</sup>, & KEIZO TAKESHITA<sup>1</sup>

<sup>1</sup>Faculty of Pharmaceutical Sciences, Sojo University, Kumamoto 860-0082, Japan, and <sup>2</sup>Graduate School of Engineering, Osaka City University, Osaka 558-8585, Japan

Accepted by Dr E. Niki

(Received 18 December 2006; revised 13 May 2007)

### Abstract

To suppress enzymatic reduction of nitroxyl group of spin probes, this study designed two new nitroxyl probes, 4-hydroxy and 4-oxopiperidine-*N*-oxyls having 4'-hydroxyspirocyclohexyl groups at the 2- and 6-positions of the piperidine ring (hydroxy-DICPO and oxo-DICPO, respectively). The decay of the EPR signal of these probes in mouse liver homogenates was significantly suppressed compared with that of 4-hydroxy- and 4-oxo-2,2,6,6-tetramethylpiperidine-*N*-oxyl (hydroxy-TEMPO and oxo-TEMPO, respectively), although hydroxy-DICPO and oxo-DICPO showed no difference in the reactivities with ascorbic acid. While both hydroxy- and oxo-DICPO reacted with hydroxyl radicals, only hydroxy-DICPO lost its EPR signal by the reaction with superoxide anion radical in the presence of cysteine. This feature is similar to that observed for hydroxy- and oxo-TEMPO. These results suggest that the introduction of spirocyclohexyl groups to nitroxyl spin probes is effective for protecting the nitroxyl group against enzymatic reduction without changing the characteristics of the reaction with oxygen radicals.

**Keywords:** Nitroxyl radical, enzymatic reduction, *in vivo* EPR, reactive oxygen species, ascorbic acid

**Abbreviations:** ROS, reactive oxygen species,  $\cdot\text{OH}$ , hydroxyl radical,  $\text{O}_2^-$ , superoxide anion radical, TEMPO, 2,2,6,6-tetramethylpiperidine-*N*-oxyl, PROXYL, 2,2,5,5-tetramethylpyrrolidine-*N*-oxyl, AsA, ascorbic acid, AAOx, ascorbate oxidase, HX, hypoxanthine, XOD, xanthine oxidase, DFO, deferoxamine mesylate, PB, 20 mM sodium phosphate buffer, pH 7.4, PBS, Dulbecco's phosphate-buffered saline, oxo-DICP, 7-aza-4,12-dihydroxy-15-oxodispiro[5.1.5.3]hexadecane, oxo-DICPO, 7-aza-4,12-dihydroxy-15-oxodispiro[5.1.5.3]hexadecane-7-yloxy, hydroxy-DICPO, 7-Aza-4,12,15-trihydroxydispiro[5.1.5.3]hexadecane-7-yloxy,  $E_{1/2}$ , mid-point potential,  $E_{pa}$ , anodic peak potential.

### Introduction

It has become clear that alterations of the redox balance by the generation of reactive oxygen species (ROS) such as hydroxy radical ( $\cdot\text{OH}$ ) and superoxide anion radical ( $\text{O}_2^-$ ) are involved in the mechanisms related to ageing and disease states such as diabetes, hypertension and arteriosclerosis [1,2]. In live animals, the measurement of variations of the redox

balance with the progress of disease is essential for clearly elucidating the relationship between ROS and disease states.

Recent progress in the *in vivo* electron paramagnetic resonance (EPR) technique has enabled non-invasive measurement of the generation of ROS in live animals [3–7]. For these studies, probes carrying nitroxyl radicals (nitroxyl probes) such as derivatives

Correspondence: Keizo Takeshita, Faculty of Pharmaceutical Sciences, Sojo University, Kumamoto 860-0082, Japan. Tel: +81-96-326-4147. Fax: +81-96-326-5048. E-mail: keizo@ph.sojo-u.ac.jp

of 2,2,6,6-tetramethylpiperidine-*N*-oxyl (TEMPO) and 2,2,5,5-tetramethylpyrrolidine-*N*-oxyl (PROXYL) have been widely used. A previous report [8] showed that both TEMPO- and PROXYL-derivatives lost their paramagnetism by the reaction with  $\cdot\text{OH}$ . However, in contrast to PROXYL-derivatives, TEMPO-derivatives other than oxo-TEMPO (Figure 1) lost their EPR signal in the reaction with  $\text{O}_2^-$  in the presence of either thiol compounds or NAD(P)H, although no signal reduction occurred in simple  $\text{O}_2^-$ -flux [8–10]. Accordingly, TEMPO-derivatives are of interest as probes for ROS detection.

*In vivo* the EPR signals of both TEMPO- and PROXYL-derivatives decay after administration to experimental animals. The half-lives of the *in vivo* EPR signal of 3-carbamoyl-2,2,5,5-tetramethylpyrrolidine-*N*-oxyl (carbamoyl-PROXYL) and hydroxy-TEMPO (Figure 1) were 7–8 min and  $\sim 1$  min, respectively, as measured at the upper abdomen of mice [11,12]. It was suggested that the TEMPO- and PROXYL-derivatives were distributed to various tissues depending on their substituents after intravenous administration [11,13,14] and were enzymatically and non-enzymatically reduced to the corresponding hydroxylamines in the parenchyma cells with a reduction of the EPR signals [11,14]. *Ex vivo* experiments performed with the tissue homogenates showed that the reduction activity was high in the liver and kidney [15]. Enzymatic reduction of nitroxyl probes was reported to be caused by cytochrome P-450 reductase in rat liver microsomes [16] and by the respiratory chain in mitochondria in cultured cells [17], while non-enzymatic reduction of the probes is mainly caused by ascorbic acid [18]. Such biological reduction of the probes interferes with the ROS detection because it is hard to measure the ROS-dependent decay of the probe signal during occurrence of the biological reduction. Therefore,

nitroxyl probes resistant to the biological reduction have been desired. However, such probes have not yet been employed.

Enzymatic reduction causes extensive *in vivo* decay of the probe signal [16]. To extend the biological half-lives of nitroxyl probes, the enzymatic reduction should be prevented. Provided that the reduction occurs at the active site on large enzyme molecules, the reduction would be suppressed by the introduction of large groups to probes to protect the nitroxyl group. In this study, two nitroxyl probes, hydroxy-DICPO and oxo-DICPO (Figure 1), were designed and their resistance against enzymatic reduction and their reactivities with ROS were evaluated and compared with those of the corresponding TEMPO-derivatives.

## Materials and methods

### Chemicals

Acetonin monohydrate was prepared according to Ma et al. [19]. 4-Hydroxy-2,2,6,6-tetramethylpiperidine-*N*-oxyl (hydroxy-TEMPO), 3-carbamoyl-2,2,5,5-tetramethylpiperidine-*N*-oxyl (carbamoyl-PROXYL), deferoxamine mesyrate (DFO), hypoxanthine (HX), xanthine oxidase (XOD, from bovine milk) and ascorbate oxidase (AAOx, from cucurbita sp.) were purchased from Sigma Chemical Co. (St. Louis, MO, USA), 4-oxo-2,2,6,6-tetramethylpiperidine-*N*-oxyl (oxo-TEMPO) from Aldrich Chemical Co., Inc. (Milwaukee, WI, USA), *n*-octanol,  $\text{H}_2\text{O}_2$  solution (30%), L-cysteine and L (+)-ascorbic acid (AsA) from Wako Pure Chemical Industries, Ltd. (Osaka, Japan) and Dulbecco's phosphate-buffered saline (PBS) from Gibco (Grand Island, NY, USA). Pure water was freshly prepared with a Barnstead NANO-pure DIAMOND™ (Dubuque, IA, USA). All other reagents were of the highest purity commercially available.

### Syntheses of oxo-DICPO and hydroxy-DICPO

**General.**  $^1\text{H}$  NMR spectra were recorded with a JEOL  $\alpha$ -400 spectrometer. Chemical shifts ( $\delta$ ) are expressed in ppm downfield from tetramethylsilane as the internal standard.

**7-Aza-4,12-dihydroxy-15-oxodispiro[5.1.5.3]hexadecane (oxo-DICP) [20–22].** Acetonin monohydrate (3.00 g, 17.4 mmol), 4-hydroxycyclohexanone (9.95 g, 87.2 mmol), finely divided anhydrous  $\text{NH}_4\text{Cl}$  (0.933 g, 17.4 mmol) and EtOH (10 mL) were mixed and stirred at 60°C for 10 h. After the mixture was cooled, EtOH (10 mL) was added and the resultant mixture was chromatographed on silica gel. Elution with 1:10 EtOH–EtOAc gave less polar organic compounds and subsequent elution with 1:5 EtOH–EtOAc gave an oxo-DICP rich fraction. After

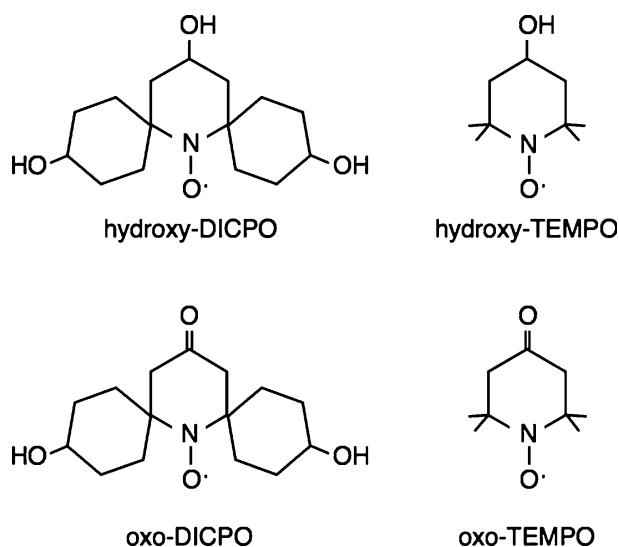


Figure 1. Structures of the nitroxyl spin probes.

the oxo-DICP rich fraction was evaporated under reduced pressure, the residual EtOH was completely removed by vacuum pumping. Washing of the residue with EtOAc gave oxo-DICP as a white powder with 19% yield (0.90 g, 3.4 mmol). Crystallization from EtOAc gave fine colourless crystals with mp 186–187°C.  $^1\text{H}$  NMR ( $\text{CD}_3\text{OD}$ )  $\delta$  = 1.36–1.95 (m, 16 H,  $\text{CH}_2\text{CH}_2\text{CH}(\text{OH})\text{CH}_2\text{CH}_2$ ), 2.35 (s,  $\text{CHHC}(\text{=O})$ , 2H), 2.45 (s,  $\text{CHHC}(\text{=O})$ , 2H), 3.57–3.69 (m,  $\text{CH}(\text{OH})$ , 2H), IR (KBr) 3313 (OH), 3222 (NH),  $1700\text{ cm}^{-1}$  (C=O). MS (EI):  $m/z$  267 ( $\text{M}^+ + 1$ ). Anal. Calcd for  $\text{C}_{15}\text{H}_{25}\text{NO}_3$ : C, 67.38; H, 9.42; N, 5.24. Found: C, 67.33; H, 9.49; N, 5.16.

*7-Aza-4,12-dihydroxy-15-oxodispiro[5.1.5.3]hexadecane-7-yloxy (oxo-DICPO)*. 3-Chloroperoxybenzoic acid (77% purity) (10 g, 45 mmol) was added to a stirred solution of oxo-DICP (1.3 g, 4.9 mmol) in EtOH (100 mL) at room temperature and the resultant mixture was stirred at room temperature for 3 days. The residue was evaporated under reduced pressure and the residue was chromatographed on alumina with 1:5 EtOH–EtOAc to give oxo-DICPO as a yellow powder with 54% yield (0.75 g, 2.7 mmol). Recrystallization from EtOAc gave fine yellow crystals with mp 171–173°C. Anal. Calcd for  $\text{C}_{15}\text{H}_{24}\text{NO}$ : C, 63.81; H, 8.57; N, 4.96. Found: C, 63.76; H, 8.56; N, 4.93.

*7-Aza-4,12,15-trihydroxydispiro[5.1.5.3]hexadecane-7-yloxy (hydroxyl-DICPO)*. A mixture of oxo-DICPO (0.100 g, 0.35 mmol) in EtOH (15 mL) was stirred until the crystals were completely dissolved. After  $\text{NaBH}_4$  (0.90 g, 24 mmol) was added, the resultant mixture was stirred for 5 h at room temperature. The unreacted  $\text{NaBH}_4$  was decomposed by the addition of acetone and the resultant mixture was further stirred at room temperature for 12 h. After filtration, the filtrate was evaporated under reduced pressure and the residue was chromatographed on alumina with 1:3 EtOH–EtOAc to give hydroxyl-DICPO with 94% yield (0.095 g, 33 mmol). Crystallization from 1:2 EtOH–EtOAc gave light red microneedles with mp 213–214.5°C. Anal. Calcd for C, 63.35; H, 9.22; N, 4.93. Found: C, 63.07; H, 9.38; N, 4.88.

#### *Determination of the n-octanol/PBS (pH 7.4) partition coefficient*

Nitroxyl probe dissolved in PBS (50  $\mu\text{M}$ , 200  $\mu\text{L}$ ) was mixed with *n*-octanol for 10 s with a vortex mixer and then the mixture was centrifuged at  $2000 \times g$  for 10 s. Both the *n*-octanol and PBS layers (17  $\mu\text{L}$  each) were separately transferred to 100- $\mu\text{L}$  disposable micropipettes (Drumond Scientific Co., Broomall, PA, USA). The micropipettes were set at a constant position in the EPR cavity and the EPR spectrum was recorded. Signal intensities were corrected with signal

of  $\text{Mn}^{2+}$  as described below. The partition coefficient was expressed as the ratio of the signal area of the *n*-octanol layer to that of the PBS layer.

#### *Electrochemical measurements*

The electrochemical measurements were carried out using a three-electrode cell. The working electrode was a glassy carbon disk (3 mm  $\phi$ , 0.071  $\text{cm}^2$  area, No. 2012, BAS, West Lafayette, IN, USA). The glassy carbon disk was polished with alumina (1  $\mu\text{m}$ ) powder on a polishing cloth and washed with distilled water before use. Reference and counter electrodes were Ag/AgCl/satd. KCl and platinum wire, respectively. The counter electrode was placed in a compartment separated from the working electrode compartment by fritted porous glass. Cyclic voltammetry was performed using a potentiostat (HAB-151, Hokuto Denko Co., Ltd, Tokyo Japan) equipped with a potential scanner. Voltammograms were recorded on a computer using a 14-bit A/D converter interface (NR-250, KEYENCE, Osaka, Japan). Voltammetric measurements were performed using aqueous solutions of nitroxyl radicals dissolved in 20 mM phosphate buffer, pH 7.4 (PB). The electrolyte was bubbled with  $\text{N}_2$  gas for 30 min before measurements. All electrochemical measurements were carried out at room temperature (ca. 25°C).

#### *Animals and animal care*

Male ddY mice (4 weeks of age) were purchased from Kyudo Co., Ltd. (Kumamoto, Japan). The mice were housed in a temperature- and humidity-controlled room and given a commercial diet (CE-2; Clea Japan, Inc., Tokyo, Japan) and water *ad libitum* until the experiment commenced. All animals used in this study were treated and handled according to the Recommendations for the Handling of Laboratory Animals for Biomedical Research compiled by the Committee for the Safety and Handling Regulations of Laboratory Animal Experiments at our university.

#### *Reduction of nitroxyl probes by liver homogenates*

After sacrifice of a mouse by cervical dislocation, the liver was immediately removed, perfused with physiological saline, weighed and homogenized in 3 mL of ice-chilled PBS per 1 g of liver with a teflon tissue grinder. After brief mixing of the liver homogenates (190  $\mu\text{L}$ ) and 0.5 mM nitroxyl probe in PBS (10  $\mu\text{L}$ ) at room temperature (24–25°C), 17  $\mu\text{L}$  of the mixture was transferred to a 100- $\mu\text{L}$  disposable micropipette (Drumond) and set at a constant position in the EPR cavity, and the decay of the EPR signal was measured at room temperature. The experiment was also performed in the presence of 12.5 U/mL AAOx.

### Reduction of nitroxyl probes by AsA

An AsA solution (2.5 mM) was prepared in fresh pure water purged with argon gas. After brief mixing of 40  $\mu\text{L}$  of the AsA solution and 160  $\mu\text{L}$  of 31.25  $\mu\text{M}$  nitroxyl probe in PB at room temperature, the mixture was immediately transferred to a quartz flat cell for EPR measurements (Labotec, Tokyo, Japan) and set at a constant position in the EPR cavity, and the decay of the EPR signal was measured at room temperature.

### Reaction of nitroxyl probes with $\cdot\text{OH}$

Hydroxy radical was generated by ultraviolet light (UV)-induced haemolytic fission of  $\text{H}_2\text{O}_2$ . A mixture of 25  $\mu\text{M}$  nitroxyl probe and 7.5 mM  $\text{H}_2\text{O}_2$  in PB was prepared in a brown vial. The mixture was transferred to a quartz flat cell and set at a constant position in the EPR cavity. Irradiation of the mixture with UV was performed in the EPR cavity with a model RUVF-203S UV-irradiation unit equipped with a 200 W mercury-xenon lamp, a UV-29 filter (cut-off: 290 nm) and a RU-330 heat ray-cut-off-filter (Radical Research, Tokyo, Japan) through a quartz fibre. Decay of the EPR signal was measured at room temperature. The competition experiment was performed in the presence of 5 mM mannitol.

### Reaction of nitroxyl probes with $\text{O}_2^-$

Forty microlitres of XOD (0.17 U/mL) were added to 360  $\mu\text{L}$  of a mixture (25  $\mu\text{M}$  nitroxyl probe, 0.5 mM HX and 20  $\mu\text{M}$  DFO with or without 0.2 mM cysteine) in PB. After a short period of stirring, the mixture was transferred to a quartz flat cell and set at a constant position in the EPR cavity. Decay of the EPR signal was measured at room temperature. Progression of HX-XOD reaction was confirmed with the production rate of uric acids, a reaction product, as the separate experiment. The concentration of uric acid was determined spectrophotometrically using the molar extinction coefficient at 290 nm,  $1.22 \times 10^4/\text{M}/\text{cm}$ .

### EPR measurement

X-band EPR spectra were recorded and analysed with a JEOL JES-FA100 EPR spectrometer (Tokyo, Japan). The amplitude of 100 kHz field modulation was 0.08 mT for hydroxy-TEMPO and carbamoyl-PROXYL, 0.02 mT for oxo-TEMPO, 0.16 mT for oxo-DICPO and 0.2 mT for hydroxy-DICPO. Signal intensity was corrected by the signal intensity of  $\text{Mn}^{2+}$  used as an internal standard of the EPR cavity. For reactivity studies, the EPR signal at lower magnetic field was recorded repeatedly. Sweep width was kept constant ( $\pm 0.84$  mT) to minimize the effect

of the difference in the line width on the sampling time of data.

## Results

### EPR spectra of DICPO nitroxyl probes in aqueous solution

The water solubility of both hydroxy-DICPO and oxo-DICPO was very high. As shown in Table I, the *n*-octanol/PB (pH 7.4) partition coefficients of the DICPO-derivatives were less than one-tenth of those of the corresponding TEMPO-derivatives and the partition coefficients for the DICPO-derivatives were also lower than that for carbamoyl-PROXYL, which is conventionally used as an *in vivo* probe.

Figure 2 shows the EPR spectra of the DICPO- and TEMPO-derivatives in PB. The signals of the DICPO-derivatives have broader line widths than those of the TEMPO-derivatives. The line width at the maximum slope of the central line ( $\Delta H_{msl}(0)$ ) and the hyperfine-coupling constant (*hfc*) of each spectrum are summarized in Table II. Table II shows that the  $\Delta H_{msl}(0)$  of hydroxy-DICPO is 2.7-times larger than that of hydroxy-TEMPO and the  $\Delta H_{msl}(0)$  of oxo-DICPO is 9.3-times larger than that of oxo-TEMPO. The  $\Delta H_{msl}(0)$  and *hfc* of oxo-DICPO are smaller than those of hydroxy-DICPO, as well as those of the TEMPO derivatives, and the *hfc*s of the DICPO-derivatives are slightly smaller than those of the corresponding TEMPO-derivatives.

### Redox potentials of DICPO nitroxyl probes

Cyclic voltammograms of the nitroxyl probes in PB were measured at pH = 7.4. The results are shown in Figure 3. On cathodic scan, the reduction peak of each probe appeared at  $-0.7$  to  $-0.5$  V vs Ag/AgCl and on reversal scan the corresponding reoxidation peak appeared at 0.3–0.5 V vs Ag/AgCl with a small magnitude. The broad and partially reversible waves of the anion/nitroxyl radical redox couple over a wide range have been generally observed for nitroxyl probes [10,23]. The mid-point potential ( $E_{1/2}$ ) of the reduction peak and the corresponding reoxidation peak was around  $-0.1$  V vs Ag/AgCl regardless of type of probes.

Table I. Partition coefficient ( $P_{o/w}$ ) of nitroxyl probes.

| Nitroxyl probe   | $P_{o/w}$       |
|------------------|-----------------|
| Hydroxy-DICPO    | $0.17 \pm 0.01$ |
| Oxo-DICPO        | $0.17 \pm 0.02$ |
| Hydroxy-TEMPO    | $3.14 \pm 0.23$ |
| Oxo-TEMPO        | $1.87 \pm 0.30$ |
| Carbamoyl-PROXYL | $0.63 \pm 0.03$ |

The *n*-octanol/PBS (pH 7.4) partition coefficients are presented as mean  $\pm$  SD of three experiments.

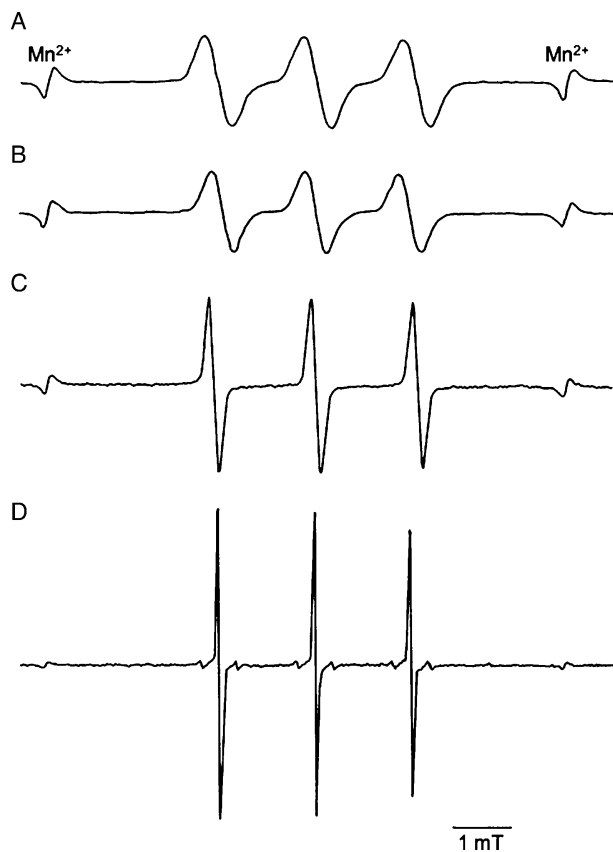


Figure 2. EPR spectra of hydroxy-DICPO (A), oxo-DICPO (B), hydroxy-TEMPO (C) and oxo-TEMPO (D) in an aqueous solution. Nitroxyl probes were dissolved in PB at a concentration of 25  $\mu\text{M}$  and EPR spectra were recorded at 0.2 mT (A), 0.16 mT (B), 0.08 mT (C) or 0.02 mT (D) of 100 kHz field modulation.

On anodic scan, the cyclic voltammograms of oxo-DICPO and oxo-TEMPO showed no rereduction peak on reversal scan (Figure 3B). On the other hand, hydroxy-TEMPO showed a reversible redox couple as reported [23] and hydroxy-DICPO exhibited a partially reversible redox couple (Figure 3A). Therefore, the oxidation property of probes was evaluated with the anodic peak potential ( $E_{pa}$ ). In the cyclic voltammogram of hydroxy-DICPO, two oxidation peaks appeared (Figure 3A). It is reasonable to think that the peak marked with an arrow is due to the second product generated from the oxidation of hydroxy-DICPO because the peak increased with a decrease in scan rate (data not shown). The  $E_{pa}$  values for oxo-DICPO (0.830 V) and hydroxy-DICPO (0.754 V) are very close to those for oxo-TEMPO (0.836 V) and hydroxy-TEMPO (0.750 V), respectively (values are potentials vs Ag/AgCl). The

Table II. EPR spectral parameters of nitroxyl probes in PB.

| Nitroxyl probe | $\Delta H_{msl}(0)$ (mT) | $hfc$ (mT) |
|----------------|--------------------------|------------|
| Hydroxy-DICPO  | 0.456                    | 1.67       |
| Oxo-DICPO      | 0.375                    | 1.58       |
| Hydroxy-TEMPO  | 0.167                    | 1.71       |
| Oxo-TEMPO      | 0.040                    | 1.61       |

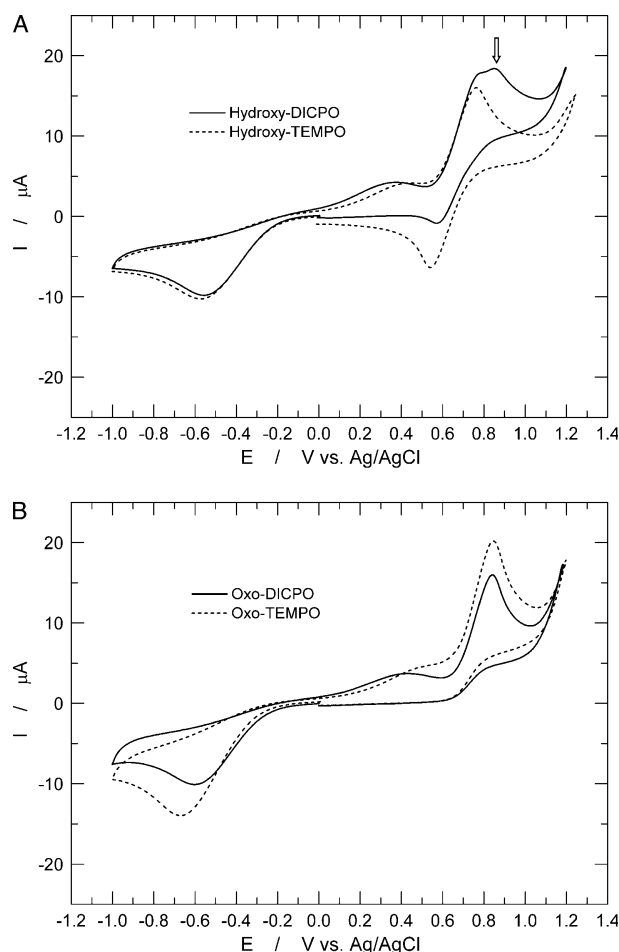


Figure 3. Cyclic voltammograms of nitroxyl probes. The cyclic voltammograms of hydroxy-DICPO and hydroxy-TEMPO (A) and oxo-DICPO and oxo-TEMPO (B) were obtained with a cathodic potential scan followed by anodic one at a rate of 20 mV/s. Concentrations of probes in PB were 2.8 mM for oxo-TEMPO and 2.1 mM for others.

$E_{pa}$  values for oxo-substituted probes were about 100 mV higher than those for hydroxy-substituted probes.

#### Stability of DICPO-derivatives in liver homogenate

Since the activity of nitroxyl-reduction was reported to be high in the liver and kidney [15], the decay of the EPR signal of the DICPO-derivatives was compared with that of the signal of the TEMPO-derivatives in the liver homogenate (Figure 4A). As previously reported, the EPR signals of the TEMPO-derivatives were reduced rapidly as compared with the signal of carbamoyl-PROXYL [15]. Interestingly, the signal decay of the DICPO-derivatives was slower than that of the corresponding TEMPO-derivatives. The signal decay of the oxo-substituted TEMPO probe was faster than that for the hydroxy-substituted TEMPO probe and a similar tendency was also observed for the DICPO-derivatives.

Liver homogenates contain AsA, which reduces nitroxyl probes [18,22]. To assess whether or not the

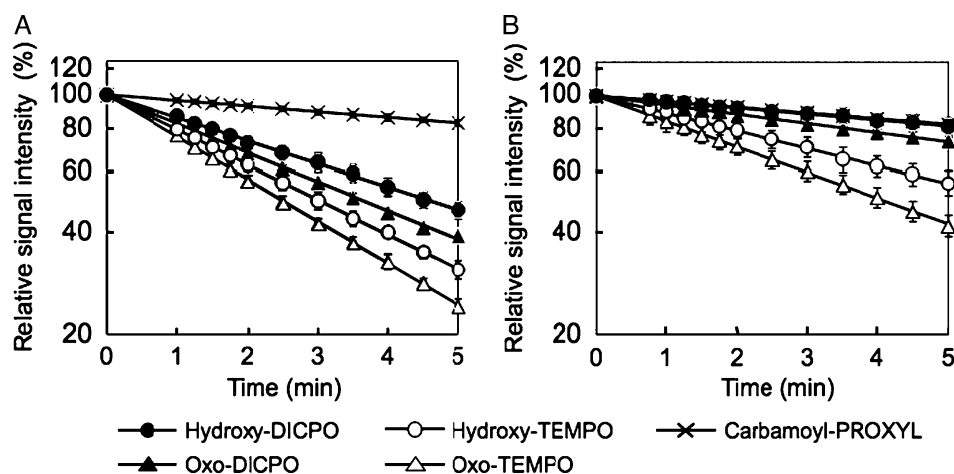


Figure 4. Signal decay of nitroxyl probes in mouse liver homogenate. The relative signal intensity of hydroxy-DICPO (closed circles), oxo-DICPO (closed triangles), hydroxy-TEMPO (open circles), oxo-TEMPO (open triangles) or carbamoyl-PROXYL (crosses) was plotted against time after mixing with mouse liver homogenate in the absence (A) or presence (B) of AAOx. Concentrations of probe, homogenate and AAOx were 25  $\mu\text{M}$ , 25 w/v% and 12.5 U/mL, respectively. Further addition of AAOx did not change the reduction rates for (B). The values are the average from three experiments and the bars indicate standard deviation.

difference in the decay rates among the probes in the homogenates resulted from the difference in the reactivity of the probes with AsA, the EPR signal decay caused by AsA was compared among the probes. As shown in Figure 5, the rates of the signal reduction of the DICPO-derivatives were almost the same as those of the TEMPO-derivatives, although the signal reduction of carbamoyl-PROXYL was very slow. This result suggests that the difference in the rate of signal decay of the DICPO- and TEMPO-derivatives in the liver homogenate depends on the difference in the resistance of the probes to enzymatic reduction. This was confirmed by the signal decay in the liver homogenate in the presence of AAOx. The presence of AAOx markedly lowered the rate of signal decay of nitroxyl probes, except for carbamoyl-PROXYL (Figure 4B). The rate of signal decay for

hydroxy-DICPO was the same as that for carbamoyl-PROXYL and the rate for oxo-DICPO was also close to that. On the other hand, the rates of signal decay for the TEMPO-derivatives were still high, although the presence of AAOx lowered the rates. These results indicate that the presence of spirocyclohexyl rings protects the nitroxyl group from reductases.

#### Reactivity of DICPO-derivatives with oxygen radicals

Hydroxyl radical was generated by UV-dependent homolytic fission of  $\text{H}_2\text{O}_2$  and the signal decay of nitroxyl probes caused by the  $\cdot\text{OH}$  was measured. Although there were some differences, all of the probes used in this study reacted with  $\cdot\text{OH}$  (Figure 6). In the TEMPO-derivatives, the signal decay of the hydroxy-substituted probe was faster than that of the oxo-substituted one. On the other hand, there was no difference between hydroxy- and oxo-DICPOs. It is worth noting that the initial rates of the signal decay of the DICPO-derivatives were approximately 2-times higher than those of the corresponding TEMPO-derivatives (Figure 6, Table III). Little signal decay occurred in the presence of mannitol, an  $\cdot\text{OH}$  scavenger (Table III), or in the absence of  $\text{H}_2\text{O}_2$  (Figure 6), indicating that the signal decay of each probe was caused by  $\cdot\text{OH}$ .

The reactivity of the DICPO-derivatives with  $\text{O}_2^-$  was examined in  $\text{O}_2^-$ -flux using the HX/XOD system. The signal of hydroxy-DICPO was reduced by  $\text{O}_2^-$  in the presence of cysteine, but that of oxo-DICPO was not reduced (Figure 7A). The decay of hydroxy-DICPO was completely inhibited by superoxide dismutase (data not shown). The difference in the reactivity of the hydroxy- and oxo-substituted DICPO-derivatives was similar to that of the corresponding TEMPO-derivatives, indicating that the reactivity of piperidine nitroxyls with  $\text{O}_2^-$  was

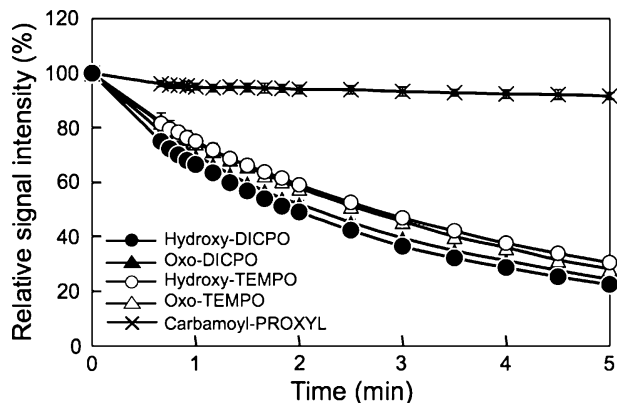


Figure 5. Signal decay of nitroxyl probes caused by AsA. Relative signal intensity of hydroxy-DICPO (closed circles), oxo-DICPO (closed triangles), hydroxy-TEMPO (open circles), oxo-TEMPO (open triangles) or carbamoyl-PROXYL (crosses) was plotted against time after mixing with AsA. Concentrations of probe and AsA were 25  $\mu\text{M}$  and 0.5 mM, respectively. The values are the average from three experiments and the bars indicate standard deviation.

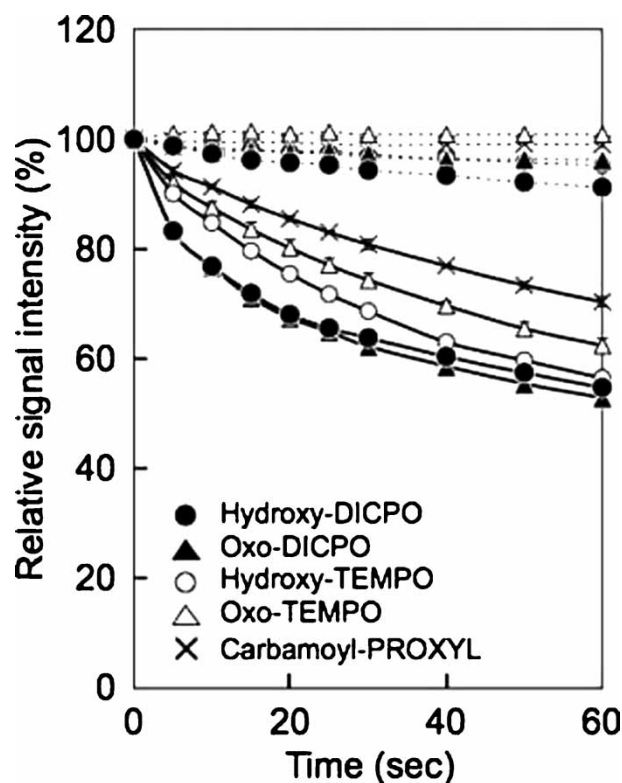


Figure 6. Signal decay of nitroxyl probes caused by  $\cdot\text{OH}$ . Aqueous solutions of 25  $\mu\text{M}$  hydroxy-DICPO (closed circles), oxo-DICPO (closed triangles), hydroxy-TEMPO (open circles), oxo-TEMPO (open triangles) and carbamoyl-PROXYL (crosses) were irradiated with UV in the presence (solid lines) or absence (dotted lines) of 7.5 mM  $\text{H}_2\text{O}_2$ . The values are the average from three experiments and the bars indicate standard deviation.

retained regardless of the presence of spirocyclohexyl rings. The presence of these probes in the HX/XOD system containing cysteine did not affect the production of uric acid (deviation:  $< 5\%$ ), which indicated that the difference in the decay rate was not due to a difference in the inhibition of the  $\text{O}_2^-$ -production system by the probes. In contrast to the large difference in the reactivities of the probes with  $\text{O}_2^-$  in the presence of cysteine,  $\text{O}_2^-$  itself did not cause any signal decay for any of the probes (Figure 7B).

Table III. Initial rate of nitroxyl decay caused by  $\cdot\text{OH}$ .

| Nitroxyl probe   | Initial rate ( $\mu\text{M/s}$ ) |                    |
|------------------|----------------------------------|--------------------|
|                  | —                                | Mannitol (5 mM)    |
| Hydroxy-DICPO    | $0.906 \pm 0.062$                | $0.137 \pm 0.016$  |
| Oxo-DICPO        | $0.894 \pm 0.024$                | $0.159 \pm 0.054$  |
| Hydroxy-TEMPO    | $0.518 \pm 0.023$                | $0.098 \pm 0.038$  |
| Oxo-TEMPO        | $0.357 \pm 0.029$                | $-0.004 \pm 0.039$ |
| Carbamoyl-PROXYL | $0.286 \pm 0.005$                | $0.022 \pm 0.018$  |

Initial rate of nitroxyl decay ( $\mu\text{M/s}$ ) was calculated from the reduction of the signal height for the initial 5 s and the initial concentration of probe (25  $\mu\text{M}$ ). Initial rates are presented as mean  $\pm$  SD of three experiments.

## Discussion

In this study, we designed hydroxy-DICPO and oxo-DICPO as new nitroxyl probes expected to be resistant to enzymatic reduction and examined their stability in liver homogenate and their reactivity with oxygen radicals. The EPR signal decay of DICPOs in liver homogenate was significantly suppressed compared with that of the corresponding TEMPO-derivatives, while no difference in their reactivity with AsA was observed. This indicates that the suppression of the reduction of DICPOs in liver homogenate was due to the acquisition of resistance to reductases. A previous study demonstrated that, while both hydroxy-TEMPO and oxo-TEMPO lost their EPR signals by reaction with  $\cdot\text{OH}$ , only hydroxy-TEMPO lost its signal by reaction with  $\text{O}_2^-$  in the presence of cysteine [8]. Similar results were observed for DICPO-derivatives, suggesting that the replacement of the methyl groups of the TEMPO-derivatives with spirocyclohexyl groups is effective for the protection of the nitroxyl group against enzymatic reduction in biological systems without interfering with the specificity of the reaction with oxygen radicals.

The  $E_{1/2}$  values of anion/nitroxyl radical couple of the DICPO- and TEMPO-derivatives were estimated to be around  $-0.1$  V vs Ag/AgCl regardless of type of the probes. Almost the same  $E_{1/2}$  of the probes coincide with the signal reduction caused by ascorbic acid. In contrast, the rates of the signal reduction of DICPO-derivatives was clearly lower than those of TEMPO-derivatives in the liver homogenate despite of the very small differences in their  $E_{1/2}$  values for the anion/nitroxyl radical couple. This indicates that the accessibility of nitroxyl moiety to the active sites of reductases is decreased in DICPO-derivatives. Since a cyclohexane ring is bulky, it is most likely that the spirocyclohexyl groups at 2- and 6-positions of the piperidine ring sterically interrupt the fit of nitroxyl moiety into the pockets of the enzyme active sites.

It is known that the enzymatic reduction of nitroxyl probes in cells is caused mainly by cytochrome P-450 reductase in microsomes and the electron transfer system in mitochondria [16,17], which are integrated in the membranes. Thus, it is likely that the active sites related to the nitroxyl reduction are localized in the hydrophobic region of the membranes. Therefore, the low *n*-octanol/PBS (pH 7.4) partition coefficient of the DICPO-derivatives may also have contributed to the resistance of the probes to those reduction systems.

The initial rates of signal decay of the DICPO-derivatives were higher than those of the TEMPO-derivatives in the reaction with  $\cdot\text{OH}$ . This suggests that the use of DICPO-derivatives makes  $\cdot\text{OH}$  detection more sensitive.

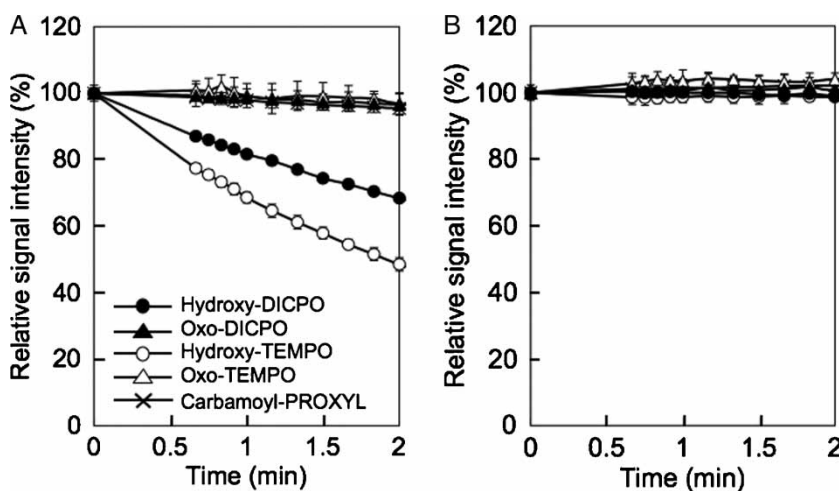


Figure 7. Signal decay of nitroxyl probes caused by  $O_2^-$ . Aqueous solutions of 25  $\mu\text{M}$  hydroxy-DICPO (closed circles), oxo-DICPO (closed triangles), hydroxy-TEMPO (open circles), oxo-TEMPO (open triangles) and carbamoyl-PROXYL (crosses) were incubated with 0.5 mM HX, 20  $\mu\text{M}$  DFO, 0.017 U/mL XOD in the presence (A) or absence (B) of 0.2 mM cysteine and relative signal heights were plotted against time. Double integrated value of signal was plotted for oxo-TEMPO, because signal height of this probe is sensitive to the amount of the dissolved oxygen which is consumed with the generation of  $O_2^-$ . The values are the average from three experiments and the bars indicate standard deviation.

In the results of reactivity of the probes with  $O_2^-$  in the presence of cysteine, the EPR signal of the oxo-substituted probes hardly decreased while the hydroxy-substituted probes showed a faster signal reduction. The electrochemical experiments show that the  $E_{pa}$  values for oxo-substituted probes were about 100 mV higher than those for hydroxy-substituted probes. This difference in the oxidation potential might be related to the difference in the reactivity between the oxo- and hydroxy-substituted probes. Unfortunately, the mechanisms related to the signal reduction of nitroxyl radical by  $O_2^-$  in the presence of cysteine are unclear at the present time.

In order to use the DICPO-derivatives as *in vivo* redox probes, two problems need to be solved; (i) the broad line width making the signal intensity insufficient for *in vivo* detection and (ii) very fast signal decay caused by AsA. If the nuclear spins of protons on the spiro rings cause the line broadening of DICPO-derivatives, perdeuteration of the probes should minimize the broadening. Furthermore, it is already known that PROXYL-derivatives are resistant to AsA, compared with TEMPO-derivatives [24,25]. This is probably due to the lower redox potential of the hydroxylamine/nitroxyl couple of PROXYL-derivatives than that of TEMPO-derivatives [23,26]. Introduction of spirocyclohexyl rings into the pyrrolidine ring of PROXYL may produce probes resistant to both enzymatic and non-enzymatic reduction. However, it should be noted that the signal reduction of PROXYL-derivatives is insensitive to  $O_2^-$ . Piperidine and pyrrolidine nitroxyls should be used appropriately depending on the oxygen radicals to be measured.

Enzymatic and non-enzymatic reduction of the nitroxyl group has imposed a limitation on the use of nitroxyl radicals as *in vivo* probes to detect oxygen radicals. This study has provided important basic data for designing probes with no such limitation and will contribute to more reliable detection of oxygen radicals by *in vivo* EPR spectroscopy.

### Acknowledgements

This work was supported by Grants-in-Aid for Scientific Research on Priority Areas 'Application of Molecular Spins' (Area No. 769, Proposal No. 15087206) and for Scientific Research (No. 17590047 and 19590050) from the Ministry of Education, Culture, Sports, Science and Technology (MEXT), Japan; and by SENTAN, JST, Japan.

### References

- [1] Halliwell B, Gutteridge JMC. Free radicals in biology and medicine. 3<sup>rd</sup> ed. New York: Oxford University Press; 1999.
- [2] Droge W. Free radicals in the physiological control of cell function. *Physiol Rev* 2002;82:47–95.
- [3] Takeshita K, Ozawa T. Recent progress in *in vivo* ESR spectroscopy. *J Radiat Res* 2004;45:373–384.
- [4] Takeshita K, Takajo T, Hirata H, Ono M, Utsumi H. *In vivo* oxygen radical generation in the skin of the protoporphyria model mouse with visible light exposure: an L-band ESR study. *J Invest Dermatol* 2004;122:1463–1470.
- [5] Utsumi H, Yamada K. *In vivo* electron spin resonance-computed tomography/nitroxyl probe technique for non-invasive analysis of oxidative injuries. *Arch Biochem Biophys* 2003;416:1–8.
- [6] Utsumi H, Takeshita K. *In vivo* ESR measurement of free radical reactions in living animals using nitroxyl probes. In: Ohya-Nishiguchi H, Packer L, editors. *Bioradicals detected*



- by ESR spectroscopy. Switzerland: Birkhäuser Verlag Basel; 1995. p 321–334.
- [7] Han JY, Takeshita K, Utsumi H. Noninvasive detection of hydroxyl radical generation in lung by diesel exhaust particles. *Free Radic Biol Med* 2001;30:516–525.
- [8] Takeshita K, Saito K, Ueda J, Anzai K, Ozawa T. Kinetic study on ESR signal decay of nitroxyl radicals, potent redox probes for *in vivo* ESR spectroscopy, caused by reactive oxygen species. *Biochim Biophys Acta* 2002;1573:156–164.
- [9] Finkelstein E, Rosen G, Rauckman EJ. Superoxide-dependent reduction of nitroxides by thiols. *Biochim Biophys Acta* 1984;802:90–98.
- [10] Krishna MC, Grahame DA, Samuni A, Mitchell JB, Russo A. Oxoammonium cation intermediate in the nitroxide-catalyzed dismutation of superoxide. *Proc Natl Acad Sci USA* 1992;89:5537–5541.
- [11] Utsumi H, Muto E, Masuda S, Hamada A. *In vivo* ESR measurement of free radicals in whole mice. *Biochem Biophys Res Commun* 1990;172:1342–1348.
- [12] Tada M, Yokoyama H, Ito O, Ohya H, Ogata T. Evaluation of the hepatic reduction of a nitroxide radical in rats receiving ascorbic acid, glutathione or ascorbic acid oxidase by *in vivo* electron spin resonance study. *J Gastroenterol Hepatol* 2004;19:99–105.
- [13] Sano H, Naruse M, Matsumoto K, Oi T, Utsumi H. A new nitroxyl-probe with high retention in the brain and its application for brain imaging. *Free Radic Biol Med* 2000;28:959–969.
- [14] Griffeth LK, Rosen GM, Rauckman EJ, Drayer BP. Pharmacokinetics of nitroxide NMR contrast agents. *Invest Radiol* 1984;19:553–562.
- [15] Couet WR, Eriksson UG, Tozer TN, Tuck LD, Wesbey GE, Nitecki D, Brasch RC. Pharmacokinetics and metabolic fate of two nitroxides potentially useful as contrast agents for magnetic resonance imaging. *Pharm Res* 1984;1:203–209.
- [16] Iannone A, Bini A, Swartz HM, Tomasi A, Vannini V. Metabolism in rat liver microsomes of the nitroxide spin probe TEMPOL. *Biochem Pharmacol* 1989;38:2581–2586.
- [17] Chen K, Morse PD 2nd, Swartz HM. Kinetics of enzyme-mediated reduction of lipid soluble nitroxide spin labels by living cells. *Biochim Biophys Acta* 1988;943:477–484.
- [18] Eriksson UG, Brasch RC, Tozer AT. Nonenzymatic bioreduction in rat liver and kidney of nitroxyl spin labels, potential contrast agents in magnetic resonance imaging. *Drug Metab Dispos* 1987;15:155–160.
- [19] Ma Z, Huang Q, Bobbitt JM. Oxoammonium salts. 5. A new synthesis of hindered piperidines leading to unsymmetrical TEMPO-type nitroxides. Synthesis and enantioselective oxidations with chiral nitroxides and chiral oxoammonium salts. *J Org Chem* 1993;58:4837–4843.
- [20] Miura Y, Nakamura N, Taniguchi I. Low-temperature 'living' radical polymerization of styrene in the presence of nitroxides with spiro structures. *Macromolecules* 2001;34:447–455.
- [21] Miura Y, Ichikawa A, Taniguchi I. Living' radical polymerization of styrene mediated by spiro ring-substituted piperidinyl-N-oxyl radicals. The effect of the spiro rings on the control of polymerization. *Polymer* 2003;44:5187–5194.
- [22] Couet WR, Brasch RC, Sosnovsky G, Tozer TN. Factors affecting nitroxide reduction in ascorbate solution and tissue homogenates. *Magn Reson Imaging* 1985;3:83–88.
- [23] Kato Y, Shimizu Y, Yijing L, Unoura K, Utsumi H, Ogata T. Reversible half-wave potentials of reduction processes on nitroxide radicals. *Electrochim Acta* 1995;40:2799–2802.
- [24] Belkin S, Mehlhorn RJ, Hideg K, Hankovsky O, Packer L. Reduction and destruction rates of nitroxide spin probes. *Arch Biochem Biophys* 1987;256:232–243.
- [25] Couet WR, Brasch RC, Sosnovsky G, Lukszo J, Prakash I, Gnewuch CT, Tozer TN. Influence of chemical structure of nitroxyl spin labels on their reduction by ascorbic acid. *Tetrahedron* 1985;41:1165–1172.
- [26] Morris S, Sosnovsky G, Hui B, Huber CO, Rao NUM, Swartz HM. Chemical and electrochemical reduction rates of cyclic nitroxides (nitroxyls). *J Pharm Sci* 1991;80:149–152.